

proportional to the circular dichroism in the line and inversely proportional to the linewidth.

More generally, an absorption line (or group of lines) can be approximated by several Lorentzian curves. The anomalous rotation is obtained by summing over contributions from all the Lorentzian components.

VI. CONCLUSION

The generalization of the linear electric susceptibility leads to a general formula for the Faraday rotation which takes all multipole transitions into account. Under electric-dipole approximation, it reduces to the well-known Kramers formula. The S -state ion of Eu^{2+} is investigated. It is found that the rotation of Eu^{2+}

which comes mainly from $S_J((4f)^7) \rightarrow P_J[(4f)^6(5d)$, etc.] transitions, can be very large while still proportional to the magnetization. The anomalous rotatory dispersion about sharp lines can also be obtained directly from the general formula.

ACKNOWLEDGMENTS

I am greatly indebted to Professor N. Bloembergen for suggesting the topic, and for his constant advice, guidance, and encouragement, without which the present work could not possibly be accomplished. I am also grateful to Professor P. Pershan and Professor J. H. Van Vleck for many stimulating conversations and for their criticism on the work.

Faraday Rotation of Rare-Earth Ions in CaF_2 . II. Experiments*

Y. R. SHEN AND N. BLOEMBERGEN

Gordon McKay Laboratory, Harvard University, Cambridge, Massachusetts

(Received 17 June 1963)

The complex rotatory power of several rare-earth ions in the CaF_2 lattice has been observed. Measurements on anomalous rotatory dispersion and concomitant circular dichroism about some spectral lines in $\text{CaF}_2:\text{Nd}^{3+}$ and $\text{CaF}_2:\text{Er}^{3+}$ crystals agree well with the theory of the preceding paper. The rotatory power of Gd^{3+} in CaF_2 in the visible range is very small. By contrast, the rotation in (Eu^{2+} , Eu^{3+}) doped CaF_2 crystals is very large and stems from the Eu^{2+} ions. The rotatory dispersion measurements show that the strong absorption lines and bands of Eu^{2+} in the visible region are responsible for the large optical rotatory power of Eu^{2+} . Gd^{3+} and Eu^{2+} are isoelectronic in structure, but the difference in their optical spectra gives rise to a significant difference in their optical rotatory power. This assertion is supported by experimental observations.

I. INTRODUCTION

THE Faraday rotation in a Eu^{3+} -doped CaF_2 crystal has been measured by Chang and Burgess.¹ They found that the crystal possessed an appreciable rotatory power, and the rotation versus magnetic field curve appeared to have some saturation effect. Since the Eu impurities in the crystal were presumably all in the trivalent state, they ascribed the rotation to the trivalent Eu ions. The ground state of Eu^{3+} is, however, a singlet 7F_0 state, and the ion has zero paramagnetic rotation. Its diamagnetic rotation arises from the Zeeman perturbation on the resonance frequencies, and on the transition matrix elements. Therefore, the observed rotation should be small, independent of temperature, and have no saturation effect.

From many reports and our own experience in growing Eu-doped CaF_2 crystals, it became apparent that the Eu impurities in the CaF_2 lattice usually exist in both the trivalent and the divalent states. The ratio of the Eu^{3+} concentration to the Eu^{2+} concentration

depends on the growing conditions, but can never be either zero or infinity. The rotation observed by Chang and Burgess might well have been caused by a residual portion of Eu^{2+} in the crystals. In this case, the Eu^{2+} ion must possess a very large rotatory power. Experiments reported in this paper confirm this. According to the theory,² Eu^{2+} may indeed have a large rotatory power in the visible range, although its structure is isoelectronic with Gd^{3+} .

The observed anomalous rotatory dispersions about sharp spectral lines of rare-earth ions in CaF_2 crystals agree very well with the theory.² Such anomalous rotations were observed in metal vapors at the end of the last century.³ No quantitative result on anomalous rotatory dispersion in solids has been reported, although J. Becquerel made an early attempt on rare-earth salts.⁴ There are of course numerous experiments on paramagnetic rotation in concentrated salts in nonabsorbing regions of the spectrum, notably by the Leiden

*This research was supported by the Advanced Research Projects Agency.

¹ S. C. Chang and J. Q. Burgess, *J. Appl. Opt.* **1**, 329 (1962).

² Y. R. Shen, *Phys. Rev.* **133**, A511 (1964), preceding paper.

³ D. Macaluso and O. M. Corbino, *Compt. Rend.* **128**, 548 (1898); *Nuovo Cimento* **8**, 257 (1898); **9**, 381 (1899).

⁴ J. Becquerel, *Le Radium* **5**, 15 (1908).

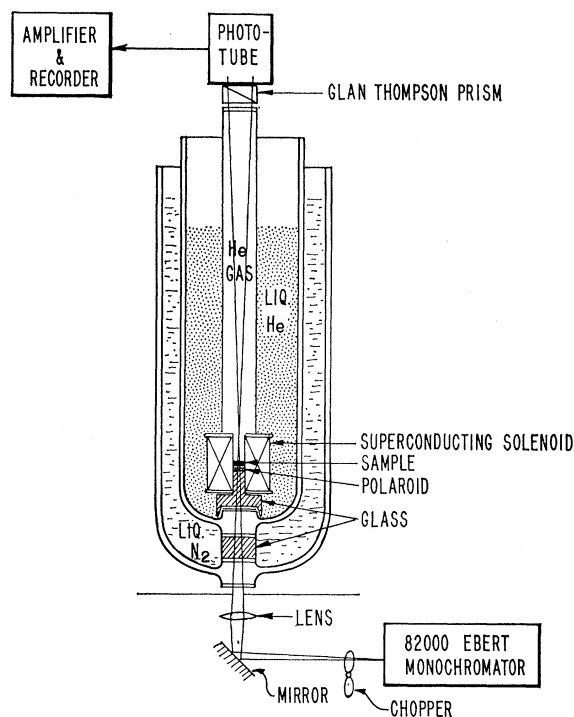


FIG. 1. The experimental setup for the measurement of Faraday rotation.

group.⁵ The availability of dilute paramagnetic crystals of optical quality, modern optical helium Dewars, and superconducting magnets, made it worthwhile to re-examine the Faraday rotation of paramagnetic ions.

II. THE EXPERIMENTAL METHOD

Rare-earth-doped CaF_2 crystals grown by the Stockbarger technique⁶ were used in our experiments, be-

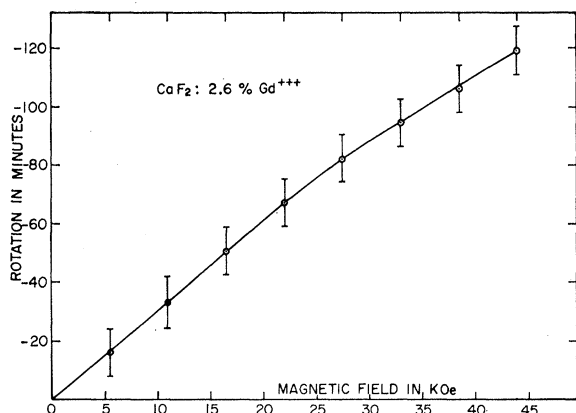


FIG. 2. Rotation versus magnetic field in $\text{CaF}_2:2.6\% \text{Gd}^{3+}$, 2 mm in length ($\lambda = 5460.7 \text{ \AA}$, $T = 4.2^\circ \text{K}$).

⁵ See, e.g., J. Van den Handel, *Encyclopedia of Physics*, edited by S. Flügge (Springer-Verlag, Berlin, 1956), Vol. 15, p. 15.
⁶ D. Stockbarger, *J. Opt. Soc. Am.* **39**, 731 (1949). The furnace was designed and built by Dr. D. A. Jones of Natural Philosophy Department, University of Aberdeen, Aberdeen, Scotland.

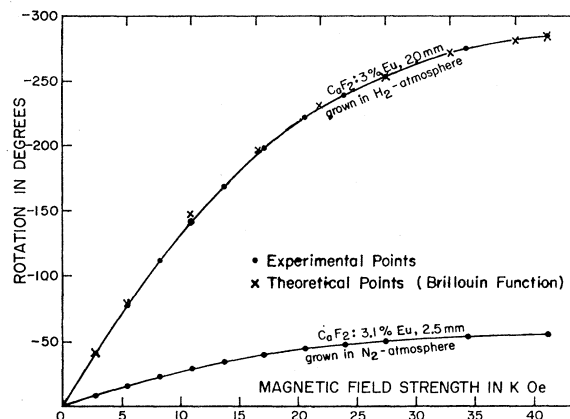


FIG. 3. Rotation versus magnetic field in $\text{CaF}_2:\text{Eu}$. ($\lambda = 5460 \text{ \AA}$, $T = 4.2^\circ \text{K}$).

cause their over-all cubic symmetry is particularly suitable for optical measurements with polarized light. However, the rare-earth ions replacing the Ca^{2+} ions in the lattice, appear both in the trivalent and divalent states. Furthermore, there exist different types of sites for the trivalent ions owing to the different possible ways of charge compensation.⁷ We may group these sites into classes, each class containing sites that are spectrally equivalent. The number of classes will be a minimum if the magnetic field is applied along a body diagonal. Therefore, in our experiments, the crystals were cut parallel to the (1,1,1) face,⁸ with the applied magnetic field perpendicular to it. The total Faraday rotation in a rare-earth-doped CaF_2 crystal is the sum of rotations due to divalent and trivalent rare-earth ions in different sites, and is, in general, not proportional to the total magnetization.

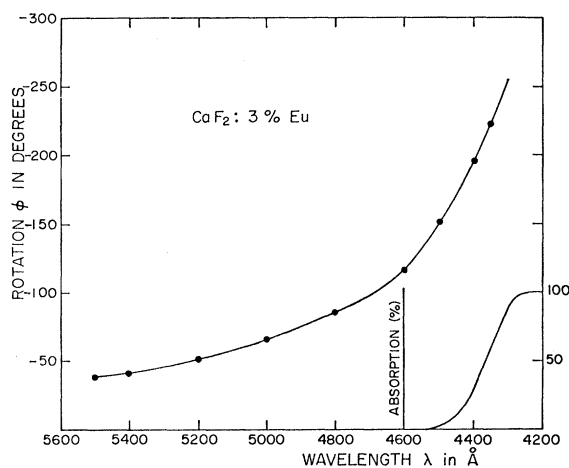


FIG. 4. Rotatory dispersion of $\text{CaF}_2:3\% \text{Eu}$, 2 mm in length, grown in hydrogen atmosphere. ($H = 2710 \text{ Oe}$, $T = 4.2^\circ \text{K}$).

⁷ M. Baker, F. Llewellyn, and D. A. Jones, *Proc. Phys. Soc. (London)* **69B**, 858 (1956); M. Baker, W. Hayes, and D. A. Jones, *ibid.* **73B**, 937 (1959).

⁸ Crystals were cut and polished by S. Maurici.

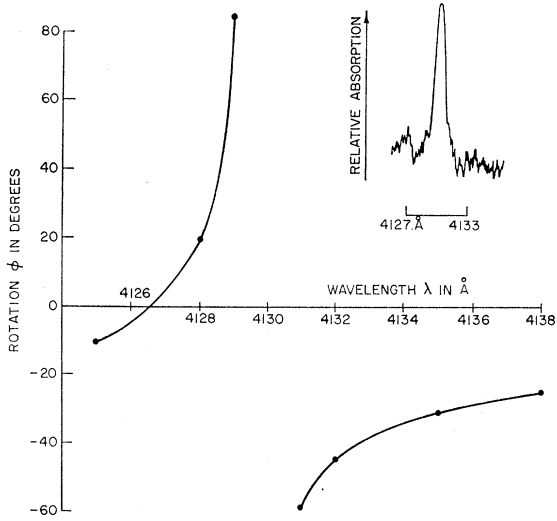


FIG. 5. Rotatory dispersion about the 4130 Å line in CaF₂:0.005% Eu, 2.5 mm in length. ($T=4.2^\circ\text{K}$, $H=13.5$ kOe).

The anomalous rotatory dispersion about a sharp line is related to the line shape and the circular dichroism of the line.² The latter quantity is defined as $Nz(f^- - f^+)$ where N is the concentration of rare-earth ions, z is the length of the light path in the sample, and f^- and f^+ are the oscillator strengths of the ion for left and right circular polarizations, respectively. The oscillator strengths can be calculated theoretically if the wave functions in the transition matrix elements are known. This has been done by Judd,⁹ who used approximate wave functions for the case of rare-earth ions in

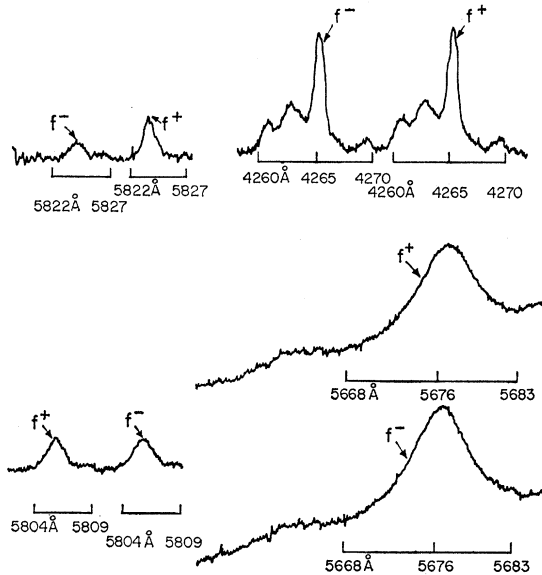


FIG. 6. Some lines of CaF₂:2.9% Nd³⁺, 2.5 mm in length at 4.2°K and 21.7 kOe. f^- and f^+ refer to left and right circularly polarized waves.

⁹ B. R. Judd, Phys. Rev. 127, 750 (1962).

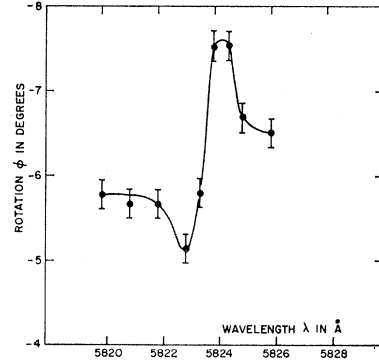


FIG. 7. Rotatory dispersion about the 5823.5-Å line in CaF₂:2.9% Nd³⁺, 2.5 mm in length. ($T=4.2^\circ\text{K}$, $H=21.7$ kOe).

liquid solutions. In the case of solids, the calculation is often very complicated owing to the crystal-field perturbation. This is particularly true for trivalent rare-earth ions in CaF₂ crystals because of the many different sites the rare-earth ions may occupy. The circular dichroism can, however, be determined directly from the experiment. When circular polarizers are used to obtain left or right circularly polarized waves, the absorption of these waves yields the circular dichroism, $Nz(f^- - f^+)$

$$= \frac{mc^2 \langle n \rangle}{\pi e^2} \left\{ \int \ln \frac{I_0}{I_-} d\left(\frac{1}{\lambda}\right) - \int \ln \frac{I_0}{I_+} d\left(\frac{1}{\lambda}\right) \right\}. \quad (1)$$

Here, $\langle n \rangle$ is the average index of refraction, λ^{-1} is the wave number in vacuum, and I_0 , I_- , and I_+ are the incoming light intensity, and the transmitted light intensities for the left and right circular waves, respectively. On reversal of the magnetic field, the following relationships hold:

$$Nz(f_{H^-} - f_{H^+}) = Nz(f_{H^-} - f_{-H^-}) = Nz(f_{-H^+} - f_{H^+}). \quad (2)$$

This property is useful in the experimental determination of circular dichroism. For a Lorentzian line,

$$\int \ln \frac{I_0}{I} d\left(\frac{1}{\lambda}\right) = \frac{\pi \Gamma}{2} \left(\ln \frac{I_0}{I} \right)_{\max}. \quad (3)$$

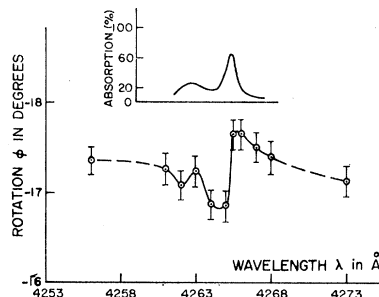


FIG. 8. Rotatory dispersion about the 4265-Å line ($^4I_{1/2} \rightarrow ^2P_{1/2}$) in CaF₂:2.9% Nd³⁺, 2.5 mm in length ($T=4.2^\circ\text{K}$, $H=21.7$ kOe).

TABLE I. Comparison of the calculated values with the measured values of the maximum anomalous rotations for four different lines in a crystal of CaF_2 with 2.9% Nd^{3+} . The rotations are the actual unnormalized rotations in the sample, 2.5 mm in length, at $T=4.2^\circ\text{K}$, in a field $H=21.7$ kOe.

Wavelength of the line λ (\AA)	Relative linewidth $\frac{\omega_{n'n}}{\Gamma_{n'n}}$	Oscillator strength $(Nz)f$	Circular dichroism $(Nz)(f^- - f^+)$	Error in determining $(Nz)(f^- - f^+)$ (%)	Maximum rotation due to the line $ \text{Re}\phi_A _{\text{max}}$ (calculated)	Maximum rotation due to the line $ \text{Re}\phi_A _{\text{max}}$ (experimental)
5823.5	5.2×10^3	2.137×10^{12}	-0.827×10^{12}	± 10	$1^\circ 17'$	$1^\circ 10' \pm 10'$
5806	3.38×10^3	4.86×10^{12}	-0.18×10^{12}	± 10	$11'$	$10' \pm 5'$
4265	4.27×10^3	2.45×10^{13}	-0.7×10^{13}	± 20	$39'$	$27' \pm 10'$
5676.5	1.09×10^3	7.18×10^{13}	$+0.74 \times 10^{13}$	± 50	$2^\circ 21'$	$1^\circ 36' \pm 10'$

The oscillator strength can then be calculated easily from the absorption maximum and the linewidth, Γ in cm^{-1} , by means of the above relation.

The experiments on Faraday rotation at helium temperature so far reported in the literature follow the old scheme of J. Becquerel.¹⁰ For an ordinary set of glass Dewars, the polarized light has to pass eight glass walls or windows and three layers of liquid. The depolarization effect of the windows, the loss of light intensity due to reflection, and the scattering of light by nitrogen and helium bubbles impair the measurements badly.

A different arrangement was used in our experiments. The complete setup is shown in Fig. 1. Here, the light beam shines up through four windows at the bottom of the Dewars and through two pieces of glass filling up the spaces below the sample in the liquid nitrogen and helium. The beam is polarized by a Polaroid sheet right in front of the sample. The sample also acts as a window that seals the lower end of the long tube in the helium Dewar, the upper end of the tube being sealed by a strain-free window at room temperature. The tube is evacuated and then filled with a small amount of He gas. The transmitted light is analyzed by a Glan-Thomson prism outside the cryostat. In this arrangement the depolarization effects and the bubble problem are effectively eliminated.

A strong magnetic field parallel to the light path is readily obtained from an air-core superconducting magnet. The Magnion magnet with 0.3-in. inside diameter

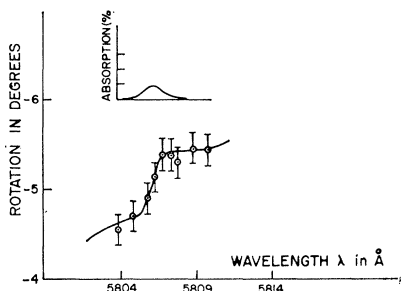


FIG. 9. Rotatory dispersion about the 5806 \AA in $\text{CaF}_2:2.9\%$ Nd^{3+} , 2.5 mm in length ($T=4.2^\circ\text{K}$, $H=21.7$ kOe).

was designed to give a maximum field of 45 kOe at 4.2°K . A combination of tungsten lamp and a Jarrell-Ash $\frac{1}{2}$ -m Ebert monochromator with a 30 000 lines per in. grating (2×2 in.²) blazed for 5000 \AA , provides a monochromatic source of variable frequency. The spectral width of the source may be regarded as an additional kind of inhomogeneous broadening to the ionic absorption line. For better sensitivity in detection, the light beam is chopped and the photocurrent is detected by a phase sensitive "lock-in" amplifier.

The rotations are obtained as averages over values corresponding to positive and negative magnetic fields. The effect of residual linear birefringence and dichroism is thus eliminated to a certain extent. The accuracy of the measurements depends on the light source, on the frequency response of the system, and on the absorbing characteristic of the sample. Under optimum conditions, the accuracy is better than 5 minutes of arc.

III. EUROPIUM IONS IN CaF_2

Gd^{3+} has been shown to possess a nearly zero paramagnetic rotatory power.¹¹ It has a ground orbital singlet $^8S_{7/2}$. The small rotatory power of Gd^{3+} in

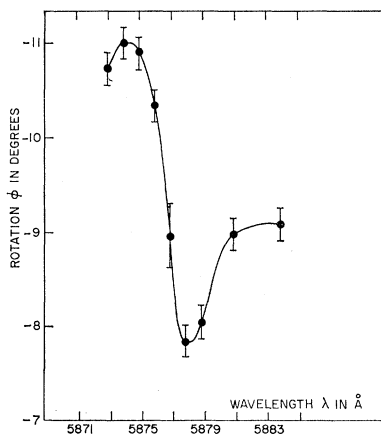


FIG. 10. Rotatory dispersion about the 5676.5- \AA line of the D group in $\text{CaF}_2:2.9\%$ Nd^{3+} , 2.5 mm in length. ($T=4.2^\circ\text{K}$, $H=21.7$ kOe).

¹¹ J. Becquerel, W. de Haas, and J. van den Handel, *Physica* 7, 711 (1940).

¹⁰ J. Becquerel, *Le Radium* 5, 6 (1908).

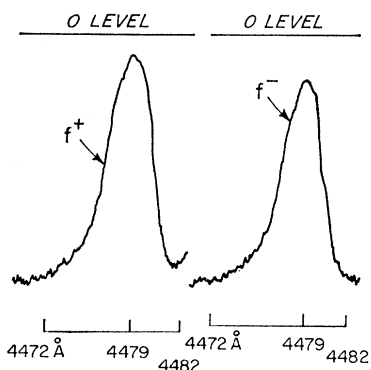


FIG. 11. Absorption curves for the 4479-Å line of $\text{CaF}_2:2\% \text{Er}^{3+}$, 2 mm in length ($T=4.2^\circ\text{K}$, $H=21.7 \text{ kOe}$).

CaF_2 is shown in Fig. 2, where the rotation versus magnetic field at 4.2°K is given for a CaF_2 crystal doped with 2.6% Gd^{3+} in molar concentration. The 5460.7-Å line of mercury was chosen as the monochromatic light, and the results were corrected for the diamagnetic rotation of the CaF_2 crystal. The paramagnetic rotation is less than 2° in a field of 43 kOe.

Two CaF_2 crystals, doped with nearly the same concentration of Eu impurities were grown under nitrogen

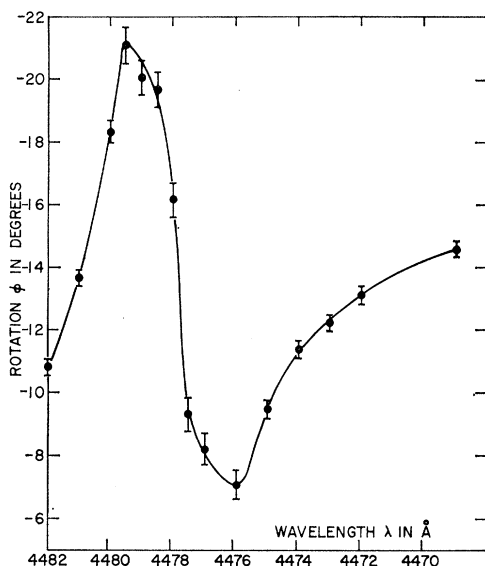


FIG. 12. Rotatory dispersion about the 4479-Å line of H group ($^4I_{15/2} \rightarrow ^4F_{5/2}$) in $\text{CaF}_2:2\% \text{Er}^{3+}$, 2.5 mm in length. ($T=4.2^\circ\text{K}$, $H=21.7 \text{ kOe}$).

and hydrogen atmospheres, respectively. The one grown in the nitrogen atmosphere has mostly Eu^{3+} impurities, whereas the one grown in the hydrogen atmosphere has mostly Eu^{2+} . This was checked by comparing the observed intensities of the Eu^{3+} spectral lines for the two species. The Faraday rotation curves are shown in Fig. 3. Clearly, the crystal with more Eu^{2+} ions has a much larger rotation. The observed rotation in the Eu-

doped CaF_2 crystals is thus attributed to Eu^{2+} ions, and is very much larger than that in Gd-doped crystals.

The experimental curve in Fig. 3 can be matched closely to a Brillouin curve. There is a very slight deviation at intermediate fields where $g\beta H$, kT , and the crystal-field splittings of the ground state¹² all have the same order of magnitude. The magnetization should also show some deviation from the Brillouin curve under these conditions. It may therefore be concluded that the rotatory power of Eu^{2+} ion is proportional to the

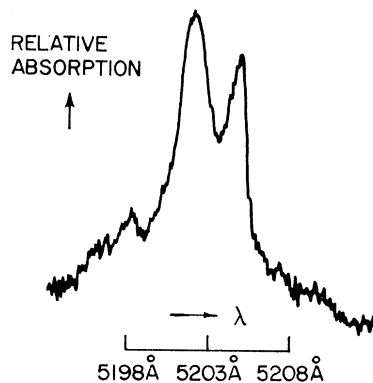


FIG. 13. A composite line of $\text{CaF}_2:2.9\% \text{Nd}^{3+}$, 2.5 mm in length ($T=4.2^\circ\text{K}$, $H=21.7 \text{ kOe}$).

magnetization of the ground state. This is compatible with the theoretical consideration, that the excited states in the strong transitions, $(4f)^7 \rightarrow (4f)^6(5d)$, etc., have $P_{5/2, 7/2, 9/2}$ character, and the cubic crystalline field splittings of these P_J states are small compared to

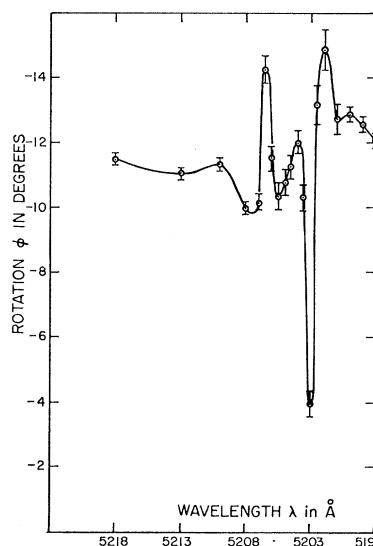


FIG. 14. Rotatory dispersion about a composite line of the E group in $\text{CaF}_2:2.9\% \text{Nd}^{3+}$, 2.5 mm in length. ($T=4.2^\circ\text{K}$, $H=21.7 \text{ kOe}$).

¹² The over-all crystal-field splitting of the ground states of Eu^{2+} is $0.1785+0.0009 \text{ cm}^{-1}$, as reported by C. Ryter, *Helv. Phys. Acta.* **30**, 353 (1957).

the separation between the J multiplets.² Otherwise, the observed proportionality between rotatory power and magnetization would be completely accidental.

The sample grown in the hydrogen atmosphere has a strong absorption band starting at 4500 Å towards the short-wavelength side. It arises from transitions between different electronic configurations $(4f)^7 \rightarrow (4f)^6 (5d)$, etc., and is the characteristic absorption of Eu^{2+} in high concentration. Figure 4 shows a rapid increase of the rotatory power as the frequency approaches the absorption band. This indicates that the strong absorption band is, to a large extent, responsible for the observed rotation.

For very dilute concentrations of Eu^{2+} in CaF_2 , the absorption starts with some narrow lines at about 4130 Å followed by absorption bands, all arising from the interconfiguration transitions $(4f)^7 \rightarrow (4f)^6 (5d)$, etc. There is a strong narrow absorption line at¹³ 4130 Å with a large oscillator strength. At frequencies close to the line, an appreciable rotatory power is expected due to the resonance effect, even though the concentration of Eu^{2+} in the crystal is low. Figure 5 shows the rotatory dispersion about the 4130-Å line of Eu^{2+} from measurements on a $\text{CaF}_2:0.005\%$ Eu crystal grown in the hydrogen atmosphere. The rotation in the region of maximum absorption could not be measured because of the large circular dichroism. The large rotation and the different signs of rotation at the two sides of the line indicate clearly that the circular dichroism of the 4130-Å line of Eu^{2+} makes an appreciable contribution to the rotatory power at frequencies near the line. In general, the strong absorption lines and bands of Eu^{2+} in the violet and near-ultraviolet region are responsible for the large optical rotation observed in Eu-doped CaF_2 crystals. One would expect to find a similar situation in crystals containing other divalent rare-earth ions.

¹³ A. A. Kaplyanskii and P. P. Feofilov, *Opt. i Spektroskopiya* **13**, 235 (1962) [translation: *Soviet Phys.—Spectry.* **13**, 129 (1962)].

IV. ANOMALOUS ROTATORY DISPERSION ABOUT SHARP SPECTRAL LINES IN RARE-EARTH-DOPED CaF_2 CRYSTALS

The theory of the preceding paper gives a relationship between the anomalous rotation about a sharp spectral line, the circular dichroism and the linewidth. Four visible spectral lines of Nd^{3+} in a $\text{CaF}_2:2.9\%$ Nd^{3+} crystal were investigated to check this relationship. The four $(4f)^3 \rightarrow (4f)^2$ intraconfiguration transitions have different oscillator strengths, different circular dichroisms, and different linewidths as shown in Fig. 6. Figures 7 to 10 give the observed anomalous rotatory dispersions about the four lines. They all have the S-shaped variation, normal or inverted, according to the sign of the circular dichroism. The first four columns in Table I give the experimental data. The circular dichroism was obtained by the method described in Sec. II. The theoretical relationship of the anomalous Faraday rotation given in the preceding paper was checked by calculating the maximum anomalous rotation $|\text{Re}\phi|_{\text{max}}$, with Eq. (31) in that paper, from the observed circular dichroism and linewidth. Comparison of the last two columns shows that theory and experiment agree within the experimental errors.

The theory was also tested for a line of Er^{3+} in a crystal of CaF_2 with 2% Er. The circular dichroism and the linewidth were obtained from the absorption curves in Fig. 11, leading to a maximum anomalous rotation of $6^\circ 42' \pm 40'$. Measurements on the anomalous rotation dispersion, shown in Fig. 12, gave an average maximum anomalous rotation of $7^\circ \pm 10'$. Here again, good agreement between theory and experiment exists.

For a line with more than one Lorentzian component, the simple S-shaped anomalous rotatory dispersion no longer obtains. The actual shape of the dispersion about such a line is obtained from the superposition of many S-shaped curves for the respective Lorentzian components. One typical example is shown in Figs. 13 and 14, where an absorption line of Nd^{3+} and the anomalous rotatory dispersion about the line are given.